Ain Shams Engineering Journal 13 (2022) 101577

Contents lists available at ScienceDirect

Ain Shams Engineering Journal

journal homepage: www.sciencedirect.com

Electrical Engineering

A novel switched model predictive control of wind turbines using artificial neural network-Markov chains prediction with load mitigation

Mahum Pervez [a,*], Tariq Kamal [b,c,d], Luis M. Fernández-Ramírez [c]

[a] University of Engineering & Technology Mardan, Pakistan
[b] School of Technology and Innovations, University of Vaasa, Vaasa FI-65101, Finland
[c] Research Group in Electrical Technologies for Sustainable and Renewable Energy (PAIDI-TEP-023), Department of Electrical Engineering, University of Cadiz, Higher Polytechnic School of Algeciras, Cadiz, Spain
[d] Department of Electrical and Electronics Engineering, Faculty of Engineering, Sakarya University, 54050 Sakarya, Turkey

ARTICLE INFO

Article history:
Received 26 November 2019
Revised 23 August 2021
Accepted 7 September 2021
Available online 23 September 2021

Keywords:
Model predictive control MPC
Finite control set
Artificial neural networks-Markov chain
ANN-MC
Load mitigation

ABSTRACT

The existing model predictive control algorithm based on continuous control using quadratic programming is currently one of the most used modern control strategies applied to wind turbines. However, heavy computational time involved and complexity in implementation are still obstructions in existing model predictive control algorithm. Owing to this, a new switched model predictive control technique is developed for the control of wind turbines with the ability to reduce complexity while maintaining better efficiency. The proposed technique combines model predictive control operating on finite control set and artificial intelligence with reinforcement techniques (Markov Chains, MC) to design a new effective control law which allows to achieve the control objectives in different wind speed zones with minimization of computational complexity. The proposed method is compared with the existing model predictive control algorithm, and it has been found that the proposed algorithm is better in terms of computational time, load mitigation, and dynamic response. The proposed research is a forward step towards refining modern control techniques to achieve optimization in nonlinear process control using novel hybrid structures based on conventional control laws and artificial intelligence.

1. Introduction

The current upgrowing energy demands with the aim of fossil fuels usage minimization, worldwide trend is shifting towards power production through renewable energy resources [1]. Wind as a renewable energy source turns out to be one of the largest contributors in the replacement of hydrocarbon fuels for electric power generation [2]. In 2016, the total electric wind power production capacity reached 486,790 MW resulting in improvement of 12.6% in contrast to the forgoing year and is estimated to reach up to 817,000 MW till year 2021 [3]. Owing to the higher demand causing continuous increase in size of wind turbines, new challenges are emerging in development of wind turbine control strategies as highlighted by [4]. For large wind turbines, the search for advance control techniques to offer optimized control having maximum energy extraction with computational efficiency is still an ongoing effort [5–8]. In wind turbine control, traditional feedback controllers respond to the effects of wind fields when they have already impacted the wind turbine. Research studies [9–11] emphasize preview control to be more encouraging towards improved operational performance especially in multi-MW scale wind turbines. However, due to strictly following power curve, excessive stress forces influence wind turbine that may result in damped modes excitation [12]. At worst, ultimate failures of wind turbines may result by undamped cyclic fatigue loads of stochastic nature due to wind turbulence [13]. Studies as [14–16] suggest that enhancement in load performance of wind turbine can be attained by usage of preview control for power production and load mitigation. Therefore preview control is utilized in this research work for optimal control of wind turbines over the entire operation region.

For performance enhancement, various advance control algorithms are applied to wind turbines based on linear-quadratic-Gaussian control (LQG) [17], fuzzy logic control [18,19], nonlinear control [20,21], maximum power point tracking (MPPT) [22–24], evolutionary algorithms [25], adaptive control [26,27], sliding

* Corresponding author: Lecturer in Electrical Engineering Department, UET Mardan Khyber Pakhtunkhwa 23200
E-mail address: maham@uetmardan.edu.pk (M. Pervez).

https://doi.org/10.1016/j.asej.2021.09.004
2090-4479/

Nomenclature

MC	Markov Chain	TPM	Transition Probability Matrix
MPC	Model Predictive Control	TP	Transitional Probability
LIDAR	Light Detection and Ranging	FNI	Forward Neighbor-hood Index
ANN	Artificial Neural Networks	BNI	Backward Neighborhood Index
ANN-MC	Artificial Neural Network-Markov Chain	ANN2	second ANN for final prediction
SMPC	Switched Model Predictive Control	MLP	Multi-Layer Perceptron
NREL	National Renewable Energy Laboratory	MAPE	Mean Absolute Percentage Error
DOF	Degrees Of Freedom	TCM	Transition Count Matrix
FAST	Fatigue Aerodynamics Structures Turbulence	MPE	Maximum Percentage Error
NMPC	Nonlinear Model Predictive Control	QF	Quality Function
ANN1	first ANN for primary prediction		

mode control [28], H_∞ control [29] and Model Predictive Control (MPC) [30–39]. Among these techniques, the most distinct feature of MPC is ability to explicitly handle the imposed constraints in optimization problem [40]. Wind turbine operation is intrinsically constrained having hard limits on generator speed, blade pitch rates and torque rates [41]. Explicit constraint handling of MPC becomes particularly beneficial in gusts and shutdown conditions. Therefore, in this work a new control technique based on MPC is deployed for effective preview control and explicit constraint handling.

In recent research, LIDAR (Light Detection and Ranging) is deployed with MPC for preview control [35,42]. LIDAR for ahead wind speed measurement has two major limitations. First, LIDAR is an uncertain device and provides very limited information about ahead wind speed [43–45]. Second, LIDAR has been in existence since 1970s but its usage at each turbine plant for preview measurements is hampered by its high cost [4]. Thus in this work, for a cost efficient solution along with maintaining efficient control, a new prediction sensor based on a hybrid model is proposed for preview control using MPC strategy.

Artificial intelligent algorithms being significantly efficient in very short term predictions (seconds or minutes ahead) [46–48] can be classified into Artificial Neural Networks (ANN) or fuzzy logic algorithms. A major limitation of fuzzy logic is its low performance in the presence of limited samples as the case of current scenario where confined samples are accessible through wind sensor i-e anemometer. Thus ANN is preferred in present application. However, using simple ANN for wind speed predictions create two major problems; First, ANN alone without a statistical model requires large number of inputs for both training and usage [49] for capturing both short and long term dynamics of wind. Second, two major causes to detroit ANN performance are [50] I) Overtraining caused through feeding large samples for capturing complete (short and long term) wind dynamics. II) Extrapolation resulted by estimation beyond experimental data. To eliminate these two issues, a statistical model is required for capturing long term (minutes to hours ahead) wind dynamics. One of the most efficient statistical techniques based on Markov Chains (MC) is utilized to form an effective hybrid model named ANN-MC for wind speed predictions forming a new prediction sensor.

A Major limitation of MPC is that it is computation intensive [34,39,51] due to solving optimization problem online at every instant. As a solution to this complication, a new control strategy based on MPC referred as Switched Model Predictive Control (SMPC) is designed constituting an offline control strategy with a finite control set applied to wind turbine to reduce computational effort along with exploiting MPC benefits.

The study uses computational efficient version of MPC that is SMPC to reduce computational burden. Also for reducing the control problem complexity, a linearized model of wind turbine is deployed at a given operating point through out the operating region. The error in prediction and the plant-model mismatch originating by the above two modifications compromises with the system and control accuracy. Various studies [52–56] utilized several optimization techniques for improving computational complexity in wide applications. In order to recover with the accuracy loss while maintaining computational efficiency, ANN-MC is used to provide optimal benefits of improvement in energy extraction while maintaining low computational burden on control algorithm [57]. The same approach has been supported by [57,58] to use preview control with MPC in wind turbine control for improving computational efficiency while maintaining the maximum energy extraction by control accuracy. Reference [59,60] demonstrates the use of neural networks in MPC control to obtain computational and time efficient control algorithms. Various recent studies[61–63] deployed neural networks in MPC control to obtain optimal performance.

Therefore, two major contributions are made in this work:

- Development of a new ANN-MC model using efficient training algorithm compared to [64] based prediction sensor for preview control to achieve the following targets.
  (a) Short term wind speed predictions (for real time optimization)
  (b) Minimization of prediction errors
  (c) Cost efficiency in contrast to costly LIDAR
  (d) Reduction in computation time
- Proposing a new SMPC strategy consisting of an offline MPC algorithm for driving the wind turbine [41] over entire operation region that incorporates the benefits of MPC in preview control along with reducing computational effort.

The paper is organized as follows: Section 2 describes modeling of wind turbine. Section 3 presents the ANN-MC prediction sensor structure and simulated test predictions.To drive the wind turbine, the proposed controller is presented in Section 4. Results of proposed controller and traditional MPC on wind turbine are compared and analyzed in Section 5. Finally, the conclusions are drawn in Section 6.

2. Wind turbine modeling

2.1. Aeroelastic model

For simulating wind turbine dynamics a baseline onshore 5 MW three bladed, variable speed and pitch controlled wind turbine developed by National Renewable Energy Laboratory (NREL) reported by [41] is considered. The aeroelastic model of the given turbine is simulated using FAST [65] with allowed Degrees Of Free-

Table 1
Available DOFs of FAST aeroelastic wind turbine model.

DOFs name	Status
First flapwise blade mode	on
Second flapwise blade mode	on
First edgewise blade mode	on
Rotor-teeter	off
Drivetrain torsional flexibility	on
Generator	on
Yaw	off
First fore-aft tower bending mode	on
Second fore-aft tower bending mode	on
First side-to-side tower bending mode	on
Second side-to-side tower bending mode	on

dom (DOF) as summarized in Table 1. Since FAST aeroelastic model does not include actuator dynamics, so their respective models as defined by (5) are also added.

2.2. Reduced nonlinear model

Complex wind turbine models such as above considered FAST [65], FLEX5 [66] or BLADED [67] are not feasible to implement in MPC due to complexity. Here, a simplified model of the above wind turbine is utilized with model equations based on [30,35]. The nonlinear rotor dynamics having aerodynamic torque T_r and thrust F_r are:

$$T_r = \frac{1}{2}\rho\pi R^3 V_r^2 \frac{C_p(\lambda,\beta)}{\lambda}$$

$$F_r = \frac{1}{2}\rho\pi R^2 V_r^2 C_T(\lambda,\beta) \tag{1}$$

where C_p is power coefficient, C_T is thrust coefficient, ρ is the density of air, R is the rotor radius, λ is tip speed ratio, β is the blade pitch angle and V_r is the relative wind speed given as:

$$V_r = V - \dot{Y}_t$$

with V as average wind speed over rotor disc and $\dot{Y}_t$ is the tower fore-aft velocity. The flexible drivetrain dynamics governing drive shaft torsion θ_Δ, rotor speed w_r and generator speed w_g are modeled as [30]

$$\theta_\Delta = \theta_r - \frac{\theta_g}{n}$$

$$\dot{w}_r = \frac{T_r}{J_r} - \frac{D_s}{J_r}\dot{\theta}_\Delta - \frac{K_s}{J_r}\theta_\Delta$$

$$\dot{w}_g = -\frac{T_g}{J_g} + \frac{D_s}{J_r n}\dot{\theta}_\Delta + \frac{K_s}{J_g n}\theta_\Delta \tag{2}$$

where T_g is generator torque, J_r is the rotor inertia, J_g is the generator inertia, n is the gearbox ratio, D_s is damping constant and K_s is torsional stiffness of drive train. θ_r and θ_g are rotor and generator angular displacements respectively. The electrical power output P_g of generator represented by a nonlinear expression as [35]

$$P_g = \eta_g T_g w_g \tag{3}$$

where η_g is the generator's electromechanical efficiency. The dynamics of turbine tower seen as 1-mass, 1-spring and 1-damper system are [35]

$$F_r = M_t\ddot{Y}_t + D_t\dot{Y}_t + K_t Y_t \tag{4}$$

where M_t, D_t and K_t are tower's mass, damping and spring constants respectively. The torque and pitch actuators are modeled as first order systems [30]

$$\dot{T}_g = -\frac{1}{\tau_g}T_g + \frac{1}{\tau_g}T_g^*$$

$$\dot{\beta} = -\frac{1}{\tau_p}\beta + \frac{1}{\tau_p}\beta^* \tag{5}$$

here τ_g and τ_p are the time constants of generator and pitch system and T_g^*, β^* are reference values for actuators' output.

2.3. Linearization

The rotor (1) and generator dynamics (3) result in a nonlinear wind turbine model. Although, various research studies [33,35] have considered Nonlinear MPC (NMPC) for turbine control which uses nonlinear models in the prediction. As a result of non-convex optimization problem, NMPC results in enhanced computational complexity and time in contrast to linear MPC. In addition, [33] concludes that NMPC provides minor improvement over linear MPC in wind turbine control performance. Therefore, a linearized model is considered for MPC scheme in this study. Linearizing Eq. (1) and (3) gives:

$$\Delta T_r \approx \frac{\partial T_r}{\partial w_r}|_{w_{ro}}\Delta w_r + \frac{\partial T_r}{\partial V}|_{V_o}\Delta V + \frac{\partial T_r}{\partial \beta}|_{\beta_o}\Delta\beta \tag{6}$$

where,

$$\frac{\partial T_r}{\partial w_r}|_{w_{ro}} = \frac{1}{2}\rho\pi R^4 \frac{V_o}{\lambda_o}\frac{\partial C_p}{\partial \lambda}|_{\lambda_o}$$

$$\frac{\partial T_r}{\partial V}|_{V_o} = \rho\pi R^3 \frac{V_o}{\lambda_o}C_{po} - \frac{1}{2}\rho\pi R^4 \frac{w_{ro}}{\lambda_o}\frac{\partial C_p}{\partial \lambda}|_{\lambda_o}$$

$$\frac{\partial T_r}{\partial \beta}|_{\beta_o} = \frac{1}{2}\rho\pi R^3 \frac{V_o^2}{\lambda_o}\frac{\partial C_p}{\partial \beta}|_{\beta_o}$$

$$\Delta F_r \approx \frac{\partial F_r}{\partial w_r}|_{w_{ro}}\Delta w_r + \frac{\partial F_r}{\partial V}|_{V_o}\Delta V + \frac{\partial F_r}{\partial \beta}|_{\beta_o}\Delta\beta \tag{7}$$

where,

$$\frac{\partial F_r}{\partial w_r}|_{w_{ro}} = \frac{1}{2}\rho\pi R^3 V_o \frac{\partial C_T}{\partial \lambda}|_{\lambda_o}$$

$$\frac{\partial F_r}{\partial V}|_{V_o} = \rho\pi R^2 V_o C_{To} - \frac{1}{2}\rho\pi R^3 w_{ro}\frac{\partial C_T}{\partial \lambda}|_{\lambda_o}$$

$$\frac{\partial F_r}{\partial \beta}|_{\beta_o} = \frac{1}{2}\rho\pi R^2 V_o^2 \frac{\partial C_T}{\partial \beta}|_{\beta_o}$$

$$\Delta P_g \approx \frac{\partial P_g}{\partial w_g}|_{w_{go}}\Delta w_g + \frac{\partial P_g}{\partial T_g}|_{T_{go}}\Delta T_g \tag{8}$$

where,

$$\frac{\partial P_g}{\partial w_g}|_{w_{go}} = \eta_g T_{go}$$

$$\frac{\partial Pg}{\partial T_g}|_{T_{go}} = \eta_g w_{go}$$

Δ shows perturbation from operating point and subscript $\bullet_o$ shows values of respective quantities at operating point determined by V_o [67]. Therefore, the linearized model can be represented as:

$$\Delta\dot{x} = \mathbf{A}\prime\Delta x + \mathbf{B}\prime\Delta u + \mathbf{E}\prime\Delta V$$

$$\Delta y = \mathbf{C}\prime\Delta x. \tag{9}$$

The system states x, system inputs u and measured outputs y are given as:

$$\Delta x = \begin{bmatrix} \Delta w_r & \Delta w_g & \Delta\theta_\Delta & \Delta Y_t & \Delta\dot{Y}_t & \Delta\beta & \Delta T_g \end{bmatrix}^T$$

$$\Delta u = \begin{bmatrix} \Delta T_g^* & \Delta\beta^* \end{bmatrix}^T$$

$$\Delta y = \begin{bmatrix} \Delta w_r & \Delta P_g \end{bmatrix}^T \quad (10)$$

For MPC, a discretized system model with sampling period T_s is obtained using zero order hold method at every time instant k.

$$x[k+1] = \mathbf{A}x[k] + \mathbf{B}u[k] + \mathbf{E}V[k] + \delta_k$$

$$y[k] = \mathbf{C}x[k] + \gamma_k \quad (11)$$

where δ_k and γ_k are functions of linearization points.

3. Proposed ANN-MC disturbance prediction sensor

For preview control, a new wind speed prediction sensor deploying a hybrid model based on artificial intelligence (ANN) and a statistical model (MC) is presented and analyzed. As shown in Fig. 1, a simple ANN1 structure with least data inputs applied is used to avoid over-training problem for accurate short term wind dynamics capture. A second order MC approach encapsulates relatively longer wind dynamics. For avoiding extrapolation, wind speed samples covering entire range are drawn to design ANN1 so that future predictions mostly involve interpolation. Wind speed data of 120 min duration from wind sensor i-e anemometer is provided to the hybrid model for design and assessment. $\widehat{v}(t+k|t)$ is primary prediction by ANN1 over prediction horizon k and i represents the i^{th} vector utilized in ANN1. Markov chain by wind samples generates a second order Transition Probability Matrix (TPM). Given primary prediction by ANN1, TPM yields corresponding Transitional Probability (TP), Forward Neighborhood Indices (FNIs) and Backward Neighborhood Indices (BNIs) representing next state probability, upper two states' and lower two states' probabilities respectively. Outputs from both ANN1 and MC are used by ANN2 for final prediction.

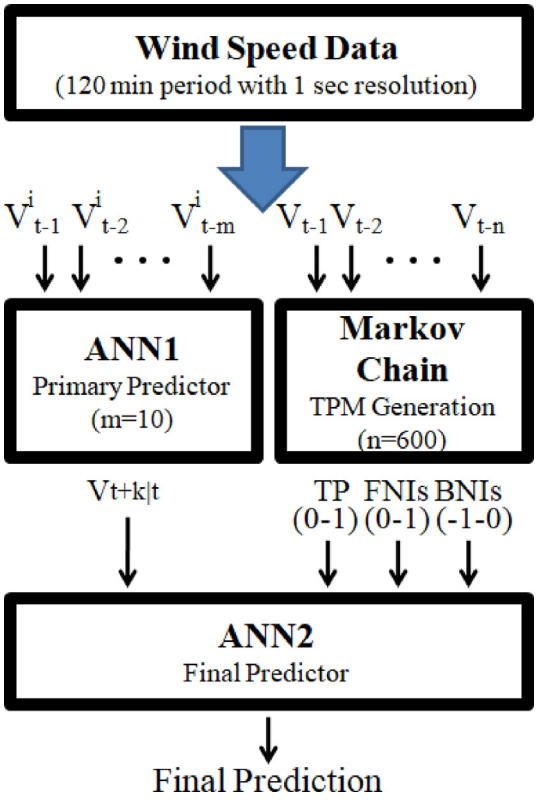

Fig. 1. Block Diagram of proposed ANN-MC disturbance prediction sensor.

3.1. ANN1 structure

The comprehensive description about different structures, relevant training algorithms and respective applications of ANN are detailed in [46–49,68–71]. For primary prediction by ANN1, one of the fastest artificial intelligence algorithm, Multi-Layer Perceptron (MLP) is deployed having a single input, hidden and output layers. The number of neurons in each layer is selected using sensitivity analysis such that minimized Mean Absolute Percentage Error (MAPE) can be achieved. Examination results in 10 neurons in input layer, 5 neurons in hidden layer and 1 neuron in output layer of ANN1 as shown in Fig. 2. For training ANN1, back-propagation algorithm is used with 30 training vectors and a learning rate of 0.25.

3.2. MC design

According to Markov's approach as utilized in various studies [72–74], the probability of the upcoming state can be derived from the previously occurred states. The order of the chain reveals the number of past steps influencing the upcoming state. Thus as suggested by [72,73] a second order MC is utilized for short term wind speed predictions in order to keep the statistical characteristics of wind preserved. For state space generation, wind speed states are derived with a step difference of 0.1 m/s to obtain higher accuracy than [72] which reported a limit difference of 1 m/s and [75] having limit difference 0.5 m/s in estimation. Given the state space with k states, corresponding Markov chain is developed with 600 wind speed data samples. Through MC, the Transition Count Matrix (TCM) is derived as follows [72]

$$TCM = \left[\eta_{i,j,k}\right]_{k^2\times k} = \begin{bmatrix} \eta_{1.1,1} & \eta_{1.1,2} & \cdots & \eta_{1.1,k} \\ \eta_{1.2,1} & \eta_{1.2,2} & \cdots & \eta_{1.2,k} \\ \vdots & \vdots & \vdots & \vdots \\ \eta_{1.k,1} & \eta_{1.k,2} & \cdots & \eta_{1.k,k} \\ \eta_{2.1,1} & \eta_{2.1,2} & \cdots & \eta_{2.1,k} \\ \eta_{2.2,1} & \eta_{2.2,2} & \cdots & \eta_{2.2,k} \\ \vdots & \vdots & \vdots & \vdots \\ \eta_{k.k,1} & \eta_{k.k,2} & \cdots & \eta_{k.k,k} \end{bmatrix} \quad (12)$$

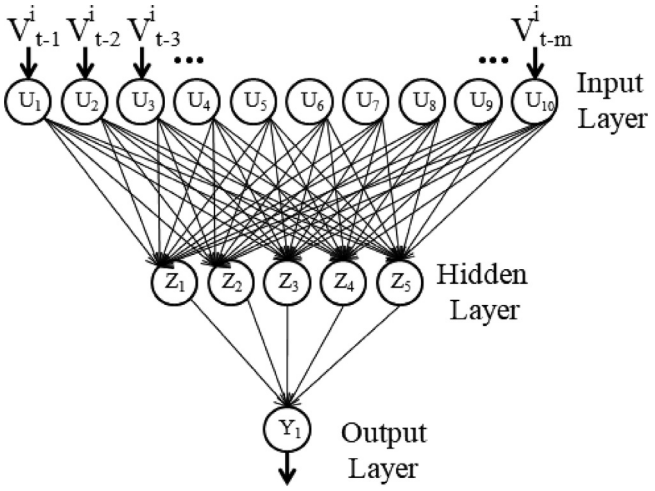

Fig. 2. Architecture of 3-Layer ANN1.

where $\eta_{i,j,k}$ is the count of moving to state k if current state is j and previous state was i. Based on TCM, second order TPM is derived giving TPs $p_{i,j,k}$ of all k states [72]

$$TPM = [p_{i,j,k}]_{k^2 \times k} = \begin{bmatrix} p_{1.1,1} & p_{1.1,2} & \cdots & p_{1.1,k} \\ p_{1.2,1} & p_{1.2,2} & \cdots & p_{1.2,k} \\ \vdots & \vdots & \vdots & \vdots \\ p_{1.k,1} & p_{1.k,2} & \cdots & p_{1.k,k} \\ p_{2.1,1} & p_{2.1,2} & \cdots & p_{2.1,k} \\ p_{2.2,1} & p_{2.2,2} & \cdots & p_{2.2,k} \\ \vdots & \vdots & \vdots & \vdots \\ p_{k.k,1} & p_{k.k,2} & \cdots & p_{k.k,k} \end{bmatrix} \quad (13)$$

3.3. ANN2 structure

For final prediction, in order to incorporate benefits of both neural networks and Markov chains, ANN2 is designed based on MLP. ANN2 has 6 neurons (primary prediction, two FNIs, two BNIs and TP) in the input layer, 3 neurons in hidden layer and 1 neuron in output layer by consideration of least MAPE as illustrated in Fig. 3. For training by back-propagation algorithm, 10 data vectors are used with learning rate of 0.25. The complete structure of ANN-MC and the processes involved in the prediction are depicted in Fig. 4.

3.4. Error performance analysis of proposed prediction sensor

For testing error performance of the wind speed prediction by the proposed sensor, a turbulent wind field using Turbsim [76] is generated having mean speed 16 m/s. The mean, standard deviation, minimum and maximum of wind speed data are 16.02 m/s, 0.9184 m/s, 13.5 m/s and 19.4 m/s respectively, as shown by Fig. 5. As a performance analysis parameter, MAPE is given as [77]

$$MAPE(k) = \frac{1}{N}\sum_{t=1}^{N}\left(\left| \frac{e(t+k|t)}{v(t+k)} \right| \times 100 \right) \quad (14)$$

where $|\bullet|$ denotes absolute value, k is prediction horizon, N represents number of predictions, $v(t+k|t)$ is the actual wind speed and $e(t+k|t)$ is prediction error.

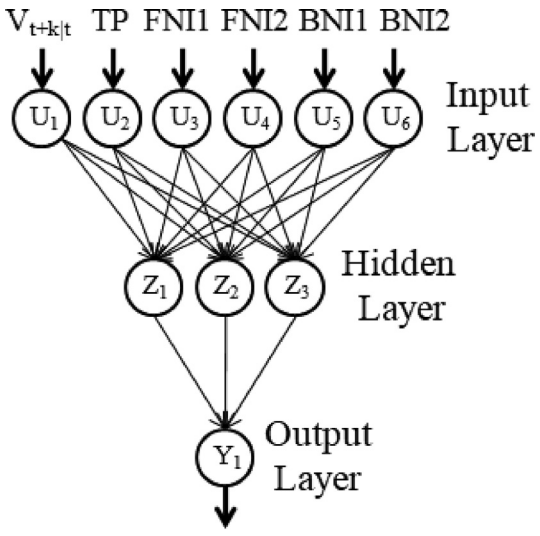

Fig. 3. Architecture of 3-Layer ANN2.

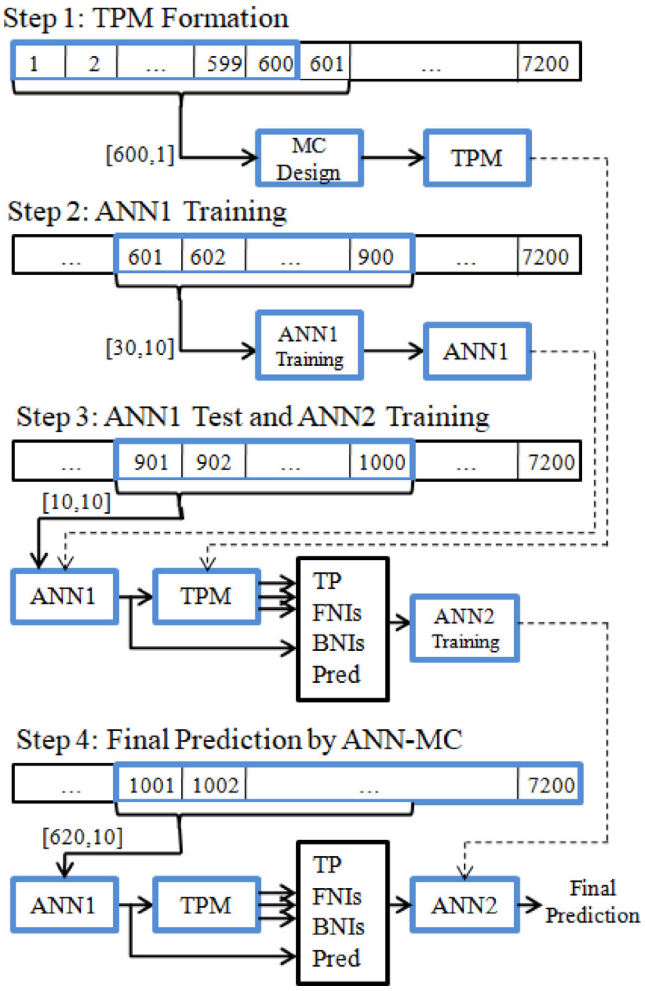

Fig. 4. Flow chart and four stages for design of proposed ANN-MC disturbance prediction sensor.

Maximum Percentage Error (MPE) is also considered as a performance analysis parameter because large MPE may lead to a wrong control command in turbine control. MPE is defined as [77]

$$MPE(k) = max\left\{ \left| \frac{e(t+k|t)}{v(t+k)} \right| \times 100 \right\}; t = 1 \ldots N \quad (15)$$

3.5. Results of ANN-MC prediction sensor

Proposed sensor is tested on 6200 wind speed samples with 1 s resolution, a section of which is shown in Fig. 5. For better resolution fourteen one step-ahead predictions by proposed sensor are highlighted in Fig. 6.

Results in Table 2 shows superior error performance in terms of MAPE and MPE of proposed ANN-MC sensor over ANN1 for prediction horizons of 1 s and 10 s.

The lower uncertainty of the proposed sensor can be deduced from Table 3 where percentage of prediction errors below $\pm 5\%, \pm 15\%$ and $\pm 30\%$ error margins are shown for both ANN1 and ANN-MC. Suggested sensor highly reduced error for higher margins.

Concluding from above results, ANN-MC prediction sensor reduces uncertainty of prediction and prediction errors. The model is trained offline (takes less than 2 s) and then can be used in online system for implementation. The final prediction by prediction sensor takes less than a millisecond thus making it feasible for the given application.

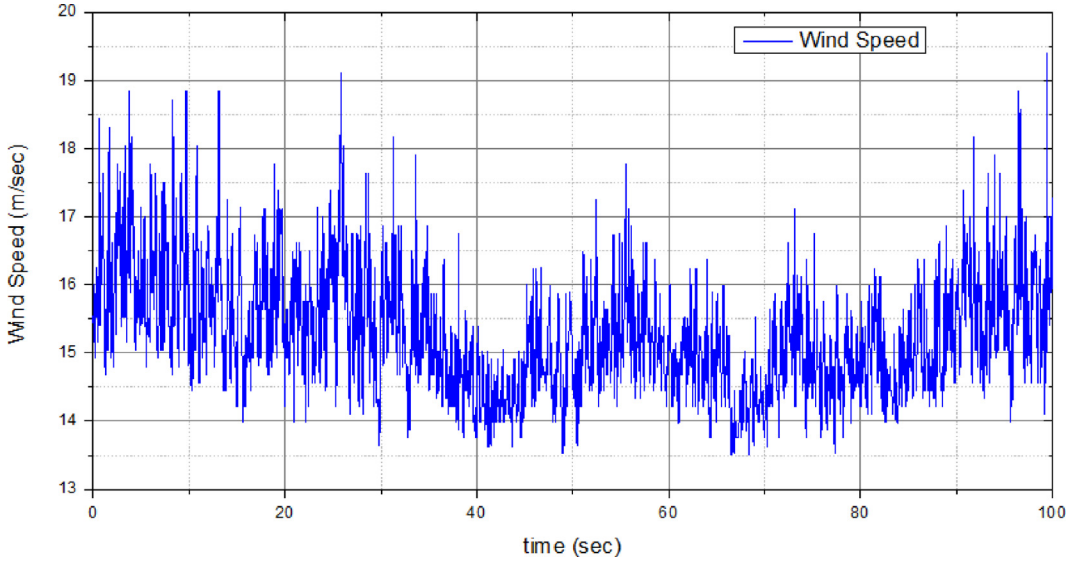

Fig. 5. Samples from stochastic wind speed data.

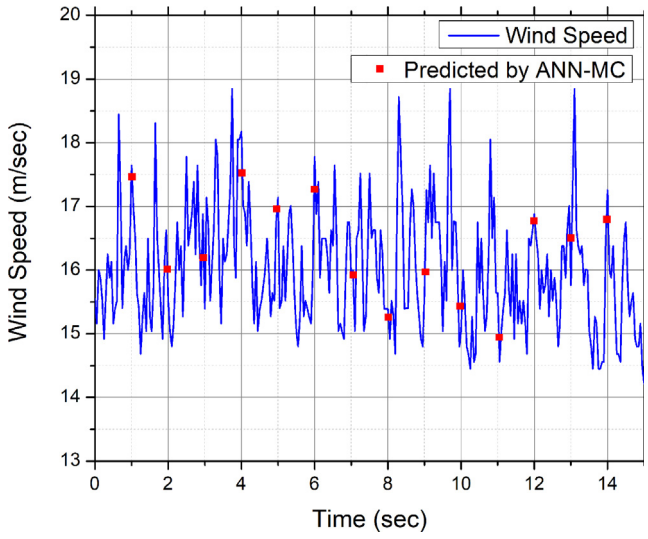

Fig. 6. Final prediction by ANN-MC prediction sensor versus actual wind speed.

4. Wind turbine controller design

4.1. Proposed switched model predictive control

4.1.1. Control strategy

The suggested control strategy is based on the idea that a finite set of feasible control outputs can be considered for driving a wind turbine plant where a prediction model outputs the behavior of the other state variables for each switching control state in the finite control set. For optimal switching control output selection, a quality function (QF) is defined. At a given operating point, each switching control output is evaluated by the defined QF. The output of the proposed controller is switched to the control output that minimizes the QF. The proposed control is designed in the following steps:

(a) Given the system model, defined by Eq. (11), finite control sets having feasible switching control outputs are generated for both actuators.
(b) A model predictor for prediction of controlled variables and a current state observer to provide the model predictor with current state estimate.
(c) A quality function is defined for selection of optimal switching control output within finite control sets at a given operating point.

The block diagram of the implemented proposed controller is presented in Fig. 7 whereas the control procedure at each sampling instant k is described as follows:

(a) The estimated wind speed $\hat{v}[k]$ from proposed ANN-MC sensor gives the reference controlled variables $r[k] = \left[w_r^*[k]\ P_g^*[k]\right]^T$.
(b) A state observer gives current state estimate $\hat{x}[k|k]$.
(c) Model predictor predicts the controlled variables $\hat{y}[k+j|k]$ over the prediction horizon for each control set $T_g^{set}[k]$ and $\beta^{set}[k]$.
(d) The QF is evaluated for each control set over prediction horizon. The control output sequence giving minimized QF is obtained among which the first optimal input $u[k|k] = \left[T_g^*[k]\ \beta^*[k]\right]^T$ is applied to the plant.

Table 2
Error performance analysis of ANN1 and ANN-MC.

Prediction horizon	ANN1		ANN-MC	
	MAPE	MPE	MAPE	MPE
t + 1	2.81	19.01	2.03	15.8
t + 10	12.21	36.01	10.9	32.56

Table 3
Error margins and confidence level of ANN1 and ANN-MC.

Error Margin	1 s		10 s	
	ANN1	ANN-MC	ANN1	ANN-MC
±5%	77.21	83.23	26.43	29.06
±15%	99.8	99.01	71.67	74.47
±30%	100	100	97.12	96.81

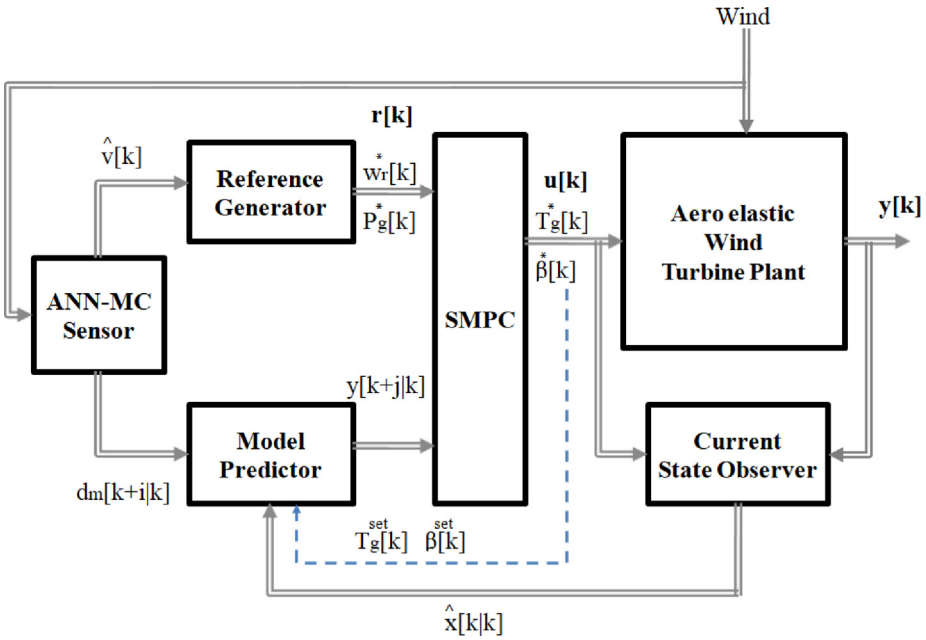

Fig. 7. Proposed Switched Model Predictive Control.

4.1.2. Finite control sets generation

In order to reduce the size of control sets, the control objective is classified into two parts. Below rated wind speed the control objective is:

$$min|w_r - w_r^{opt}|,\ min|P_g - P_g^{opt}|$$

$$\text{s.t}\ \left\{T_g \in \left[0 \quad T_g^{rated}\right], \beta = \beta^{opt}\right\}$$

where $\bullet^{opt}$ denotes the optimal values of respective quantities at an operating point. Whereas at above rated wind speed the control objective is:

$$min|w_r - w_r^{rated}|,\ min|P_g - P_g^{rated}|$$

$$\text{s.t}\ \left\{T_g = T_g^{rated}, \beta \in \left[\beta^{min}\ \beta^{max}\right]\right\}$$

with $\bullet^{rated}$ shows the rated values of respective quantities. In terms of motion rates, imposed by the constraints specified by [41] the permissible actuator actions applied by controller can be summarized as:

$$\dot{T}_g^* \in \left[\dot{T}_g^{min}\ \dot{T}_g^{max}\right], \dot{\beta}^* \in \left[\dot{\beta}^{min}\ \dot{\beta}^{max}\right]$$

Thus the number of switching control states in torque and pitch control sets respectively are calculated as:

$$m = \frac{\dot{T}_g^{max} - \dot{T}_g^{min}}{\dot{T}_{g\Delta}}$$

$$n = \frac{\dot{\beta}^{max} - \dot{\beta}^{min}}{\dot{\beta}_\Delta} \tag{16}$$

here $\bullet_\Delta$ represents the minimal variation in respective motion rates.

4.1.3. Current state observer

Since all the state variables are not available at the output, so a current state observer is designed as shown in Fig. 8. Given the

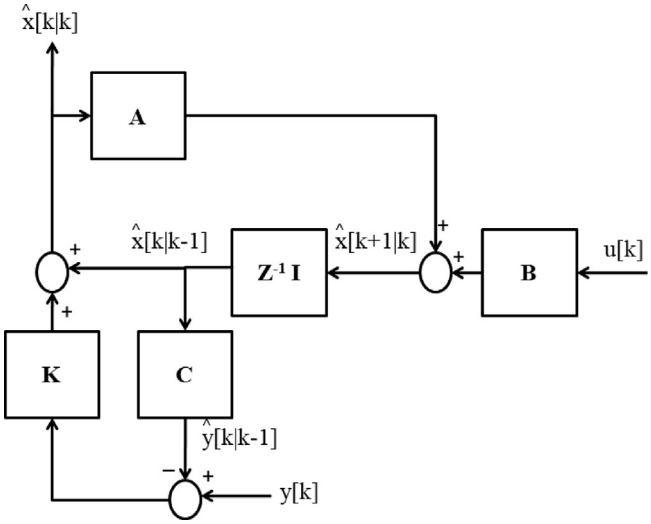

Fig. 8. Current State Observer.

model (11) at an operating point with the plant's input $u[k]$ and output $y[k]$ applied, the observer estimates the current state of the plant $\hat{x}[k|k]$ at instant k.

$$\hat{x}[k|k] = \hat{x}[k|k-1] + K(y[k] - \hat{y}[k|k-1])$$

$$\hat{x}[k+1|k] = A\hat{x}[k|k] + Bu[k]$$

$$\hat{y}[k|k-1] = C\hat{x}[k|k-1] \tag{17}$$

The observer gain K is designed using Kalman filtering technique in [78].

4.1.4. Model predictor

SMPC uses (11) to predict the controlled variables over the prediction horizon H_p. Model predictor deploys predicted wind over H_p from proposed ANN-MC sensor, which is added as measured disturbance d_m in the prediction model to make accurate estimations. Prediction step is given as:

$$\hat{x}[k+j|k] = A^j \hat{x}[k|k] + \sum_{i=0}^{j-1} A^{j-i-1} Bu[k+i|k] + \sum_{i=0}^{j-1} A^{j-i-1} Ed_m[k+i|k] \; \hat{y}[k+j|k] = C\hat{x}[k+j|k] \; , j = 1 \ldots H_p \tag{18}$$

4.1.5. Quality function

Based on the control objectives, quadratic quality functions (QFs) are defined in this work. Since the control problem is divided into two parts each handling one actuator so two QFs are defined to fulfill the complete control objective. Given the predicted controlled variables, their respective references, the QF is evaluated for each switching control output in control sets over prediction horizon H_p. The sequence minimizing the QF is obtained of which the first input $u[k] = u[k|k]$ is applied to the plant. The QFs, each incharge of separate actuators are defined as:

$$QF_1 = \sum_{j=k}^{k+H_p-1} (y[j+1|k] - r[j+1|k])^T Q_{e1} (y[j+1|k] - r[j+1|k]) + \sum_{j=k}^{k+H_p-1} \Delta T_g^*[j|k]^T R_{u1} \Delta T_g^*[j|k] \tag{19}$$

$$QF_2 = \sum_{j=k}^{k+H_p-1} (y[j+1|k] - r[j+1|k])^T Q_{e2} (y[j+1|k] - r[j+1|k]) + \sum_{j=k}^{k+H_p-1} \Delta \beta^*[j|k]^T R_{u2} \Delta \beta^*[j|k] \tag{20}$$

where Q_e and R_u are weighting matrices.

4.1.6. Constraints

Since the actuator actions are constrained by hardware limitations so their permissible actions and permissible outputs are taken in account for finite control sets generation such that:

$\Delta T_g^{min} \leqslant \Delta T_g^*[j|k] \leqslant \Delta T_g^{max}$ and

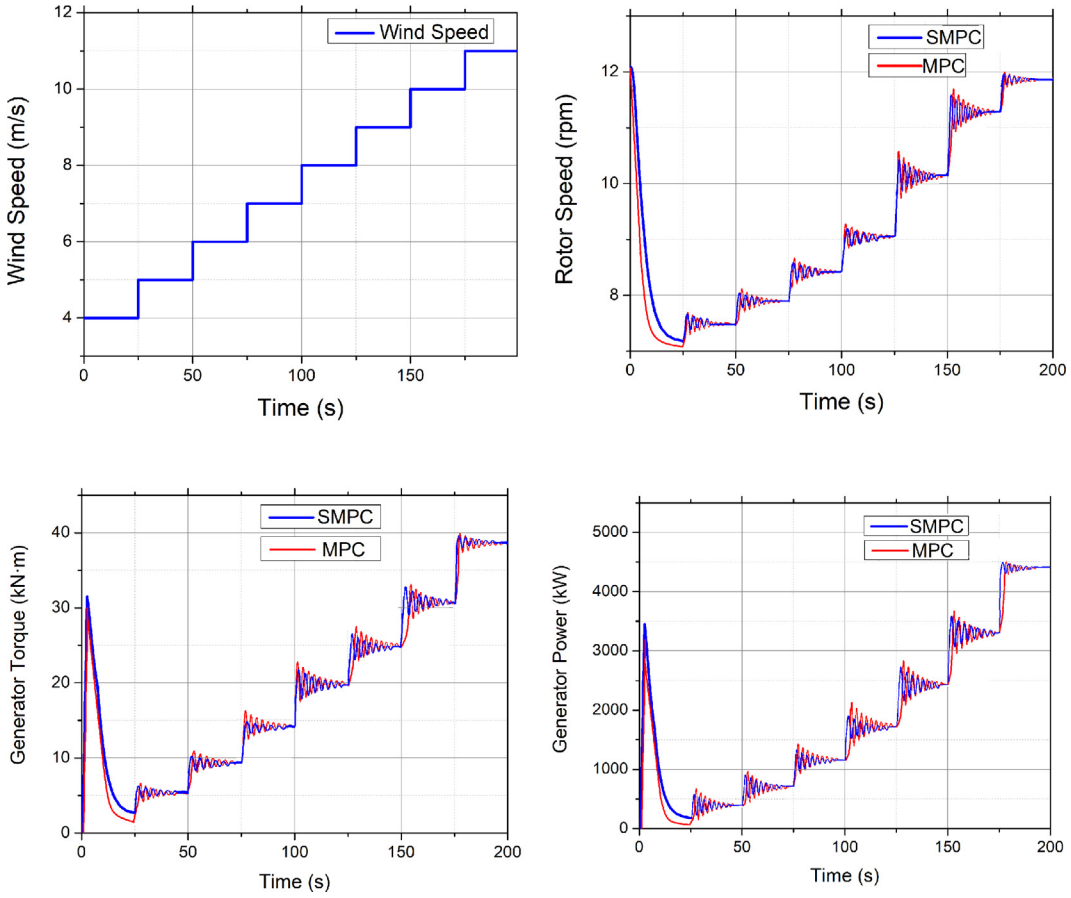

Fig. 9. Wind Power Plant Characteristics in optimal speed tracking region. (a) Wind speed versus time (b) Rotor Speed versus time (c) Generator Torque versus time (d) Generator Power versus time.

$$\Delta\beta^{min} \leqslant \Delta\beta^{*}[j|k] \leqslant \Delta\beta^{max}, j = k \ldots k + H_p - 1$$

here,

$$\Delta T_g^{*}[k] = T_g^{*}[k] - T_g^{*}[k-1]$$

$$\Delta\beta^{*}[k] = \beta^{*}[k] - \beta^{*}[k-1]$$

Given T_s and actual motion rate limits $\left\{\dot{\beta}^{min}, \dot{\beta}^{max}\right\}$ and $\left\{\dot{T}_g^{min}, \dot{T}_g^{max}\right\}$ the limits $\left\{\Delta\beta^{min}, \Delta\beta^{max}\right\}$ and $\left\{\Delta T_g^{min}, \Delta T_g^{max}\right\}$ can be obtained. The control sets are generated in consideration that the limitations on controlled variables are also fulfilled:

$$w_r[j+1|k] \leqslant w_{rmax}, j = k, k+1, \ldots, k + H_p + 1$$

$$P_g[j+1|k] \leqslant P_{gmax}$$

In addition the speed tracking and actuator relevant fatigue load is also taken into account by adjustment of weighting factors.

5. Simulation results and analysis

5.1. Under ideal wind speed steps

5.1.1. Optimal speed tracking region

The proposed strategy is simulated for ideal wind steps within lower wind region 4 m/sec to 11 m/sec and the results against traditional MPC are highlighted in Fig. 9. Comparing the results of both control strategies for performance parameters Rotor Speed

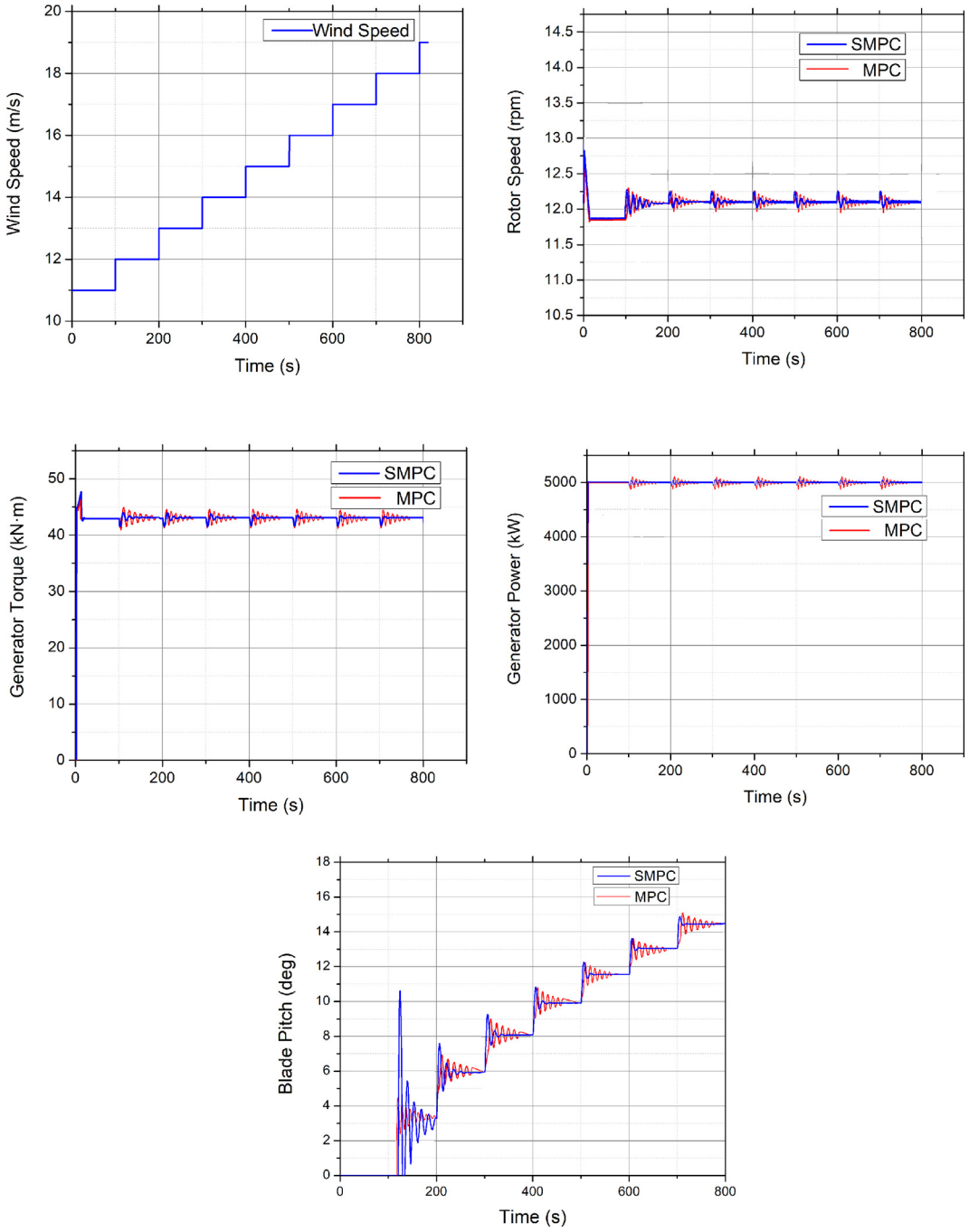

Fig. 10. Wind Power Plant Characteristics in rated speed region. (a) Wind speed versus time (b) Rotor Speed versus time (c) Generator Torque versus time (d) Generator Power versus time (e) Blade Pitch versus time.

w_r, Generator Torque T_g and Generator Power P_g, SMPC shows a faster dynamic response compared to MPC. This shows that due to faster tracking, SMPC is able to maintain improved tracking of optimal tip speed ratio $\lambda_{opt} = 7.55$. Thus SMPC provides better optimal speed tracking compared to MPC in below rated wind speed region.

Table 4
Specifications of applied Turbsim wind field.

Time step	0.01 s
Grid height	145 m
Grid Width	145 m
Mean wind speed at hub height	16 m/s
Turbulent intensity	80%

5.1.2. Rated speed region

In the above rated wind speed region 11 to 25 m/ sec both the controllers are tested with the performance illustrated in Fig. 10. While both the controllers offer satisfactory performance, SMPC due to lower computational burden due to finite control set offers a much faster response and has considerably less transient region. This property helps the SMPC to effectively maintain the rotor speed at rated value of $w_r = 12.1$ rpm. This property is specially effective to better cope with turbulent winds by keeping the power at optimal value and thus reducing extreme load conditions.

5.2. Under turbulent wind speed

In this section, the effectiveness of SMPC for load reduction due to preview control provided by ANN-MC predictions is presented.

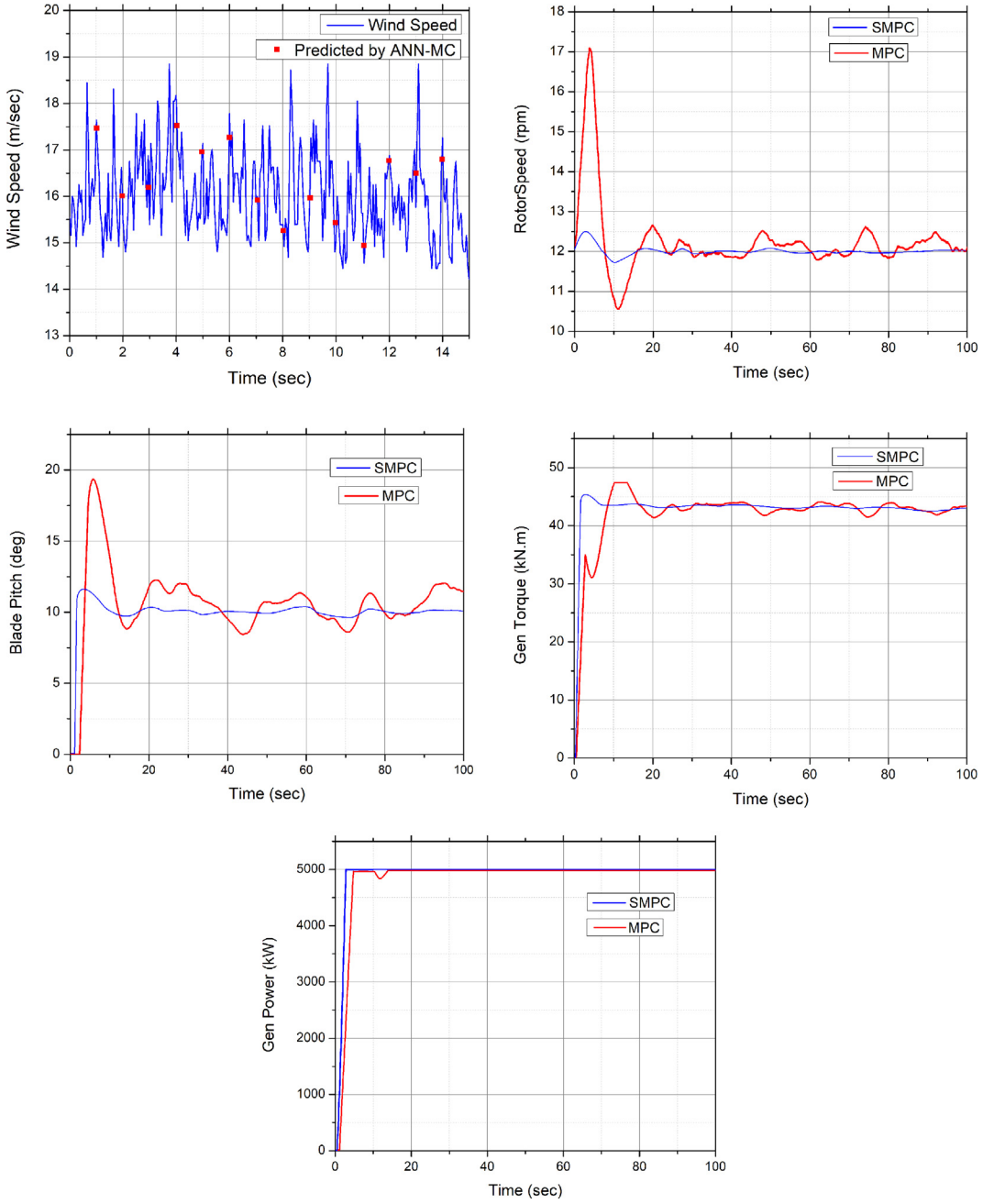

Fig. 11. Wind Power Plant Characteristics in rated speed region. (a) Wind speed versus time (b) Rotor Speed versus time (c) Blade Pitch versus time (d) Generator Torque versus time (e) Generator Power versus time.

A turbulent wind field having stochastic properties using Turbsim [76] is generated with specifications highlighted in Table 4. The resulting turbulent wind speed with ANN-MC predictions per second are indicated in Fig. 11. The wind field samples are trained over 30 training vectors from the wind field and tested over the portion indicated in Fig. 11. It is analyzed by the control plots of Fig. 11 that the SMPC due to better estimation by ANN-MC can reduce rotor speed variations with less pitch activity. This result provides SMPC special improvement over traditional MPC for better control and load reductions in real winds. The ANN-MC reduces the influence of wind disturbance to rotor speed. Thus the resultant control algorithm successfully improves control over detailed aeroelastic model of wind turbine with reduced load, improved computation time and faster dynamic response.

5.3. Reduction of computational time complexity

5.3.1. Training time of prediction model ANN-MC

The training time taken by the disturbance prediction sensor ANN-MC for various prediction horizons is given below in Table 5. Thus the time taken by the sensor is less than 2*sec* for network training and TPM calculations. The training has been performed by a conventional PC therefore the process do not required any special system performance specifications making it optimal for remote applications.

5.3.2. Overall computational efficiency of the proposed SMPC control system

After training, the trained model has been used for the disturbance predictions in the real time control system process. The average time taken by ANN-MC for final prediction is up to 0.5*msec*. The overall efficiency of the proposed control system is highlighted by defining the following speed performance analysis parameters to show the overall computational time efficiency of the system:

$$AverageSpeedFactor, SF_{avg} = \frac{(T_{avg})_{MPC}}{(T_{avg})_{SMPC}} \quad (21)$$

The average speed factor is the ratio between average time taken by the online conventional MPC $(T_{avg})_{MPC}$ to average time taken by proposed offline finite control set based SMPC $(T_{avg})_{SPMC}$. This index demonstrates the computation speed improvement by the proposed algorithm SMPC as compared to conventional MPC on average.

$$MinimumSpeedFactor, SF_{min} = \frac{(T_{max})_{MPC}}{(T_{max})_{SMPC}} \quad (22)$$

The minimum speed factor is the ratio between maximum time consumed by the online conventional MPC $(T_{max})_{MPC}$ to maximum time taken by proposed offline finite control set based SMPC $(T_{max})_{SMPC}$. This index demonstrates the computation speed improvement by the proposed algorithm SMPC as compared to conventional MPC in worst case scenario. The overall average and minimum speed factors for the conventional MPC and proposed SMPC is highlighted in Table 6. The indices of $SF_{avg} = 7$ and $SF_{min} = 3$ demonstrates that the proposed control system based on SMPC is seven times faster on average scale and three times faster in worst case compared to conventional MPC.

Table 5
Prediction horizons versus training time for ANN-MC.

Prediction Horizon	Time Response (s)
1 s	1.78
10 s	1.98

Table 6
Computation time efficiency of proposed SMPC compared to conventional MPC

Average Speed Factor SF_{avg}	Minimum Speed Factor SF_{min}
7	3

6. Conclusion

This paper presented a new hybrid technique based on modern control and artificial intelligence techniques to solve wind turbine control problem to providing faster response with reduced complexity. The control algorithm uses a finite control set to solve optimization problem reducing computational burden as compared to conventional MPC. The algorithm uses a new ANN-MC sensor for prediction of wind speed to provide efficient control output.

The observed results comparing traditional MPC with SMPC provides the following insights:

- In the optimal wind speed tracking region, the proposed control algorithm shows improved dynamic response due to faster tracking maintaining optimal tip speed ratio over entire operating region.
- In the rated speed region, the SMPC due higher computational efficiency due to finite control set and offline implementation offers a much faster response and has considerably less transient region. The improvement provides reduction in extreme load conditions in dynamic turbulent real time wind fields and gusts.
- SMPC due to better estimation by ANN-MC was able to reduce rotor speed variations with relatively lower actuator activity. The aforementioned improvement provides load mitigation ability to the wind turbine control. The ANN-MC sufficiently reduces the influence of wind disturbance to rotor speed.

The proposed control algorithm applied to the field of renewable energy promotes the advancement of wind power plant control techniques ensuring better energy extraction, stable power production due to faster dynamic response using modern control working with effective artificial intelligence techniques. The future work of the study may involve the overall cost analysis to estimate the total operating costs reduction due to load mitigation and the predicted profit due to improved energy extraction by the deployed technique in a wind farm control. The inclusion of the ability of fault diagnostics in the proposed control algorithm to improve the system robustness is also worth exploration.

Declaration of Competing Interest

The authors declare that they have no known competing financial interests or personal relationships that could have appeared to influence the work reported in this paper.

References

[1] Moriarty Patrick, Honnery Damon. What is the global potential for renewable energy? Renew Sustain Energy Rev 2012;16(1):244–52.
[2] De Vries, Bert JM, Van Vuuren, Detlef P, Hoogwijk, Monique M. Renewable energy sources: Their global potential for the first-half of the 21st century at a global level: An integrated approach. Energy Policy 2007;35(4):2590–610.
[3] Global Wind Report 2016-Annual Market, Update.report. GWEC [Online]. Available: www.gwec.net [3 July 2017].
[4] Njiri, Jackson G. Soffker Dirk, "State-of-the-art in wind turbine control: Trends and challenges. Renew Sustain Energy Rev 2016;60:377–93.

[5] Abdelbaky Mohamed Abdelkarim, Liu Xiangjie, Jiang Di. Design and implementation of partial offline fuzzy model-predictive pitch controller for large-scale wind-turbines. Renew Energy 2020;145:981–96.
[6] Luna Julio, Falkenberg Ole, Gros Sebastien, Schild Axel. Wind turbine fatigue reduction based on economic-tracking NMPC with direct ANN fatigue estimation. Renew Energy 2020;147:1632–41.
[7] Nguyen, Hoach The, Ameena Saad Al-Sumaiti, Van-Phong Vu, Ahmed Al-Durra, Ton Duc Do. Optimal power tracking of PMSG based wind energy conversion systems by constrained direct control with fast convergence rates. Int J Electr Power Energy Syst 2020;118:105807.
[8] Nouriani Ali, Moradi Hamed. Smooth switching in power control of wind turbines using a combination strategy of hysteresis and modified middle regions. Sustain Energy Technol Assessm 2020;37:100585.
[9] Laks Jason H, Pao Lucy Y, Wright Alan D. Control of wind turbines: Past, present, and future. In: Proceedings of American Control Conference. p. 2096–103.
[10] Laks J, Pao L, Wright A, Kelley N, Jonkman B. The use of preview wind measurements for blade pitch control. Mechatronics 2011;21(4):668–81.
[11] Schlipf D, Schuler S, Allgower F, Kuhn M. Look-ahead cyclic pitch control with lidar. In: Proc. of Torque.
[12] Licari John, Ugalde-Loo Carlos E, Ekanayake Janaka B, Jenkins Nicholas. Damping of torsional vibrations in a variable-speed wind turbine. IEEE Trans Energy Convers 2013;28(1):172–80.
[13] Stol KA, Zhao W, Wright, Alan D. Individual blade pitch control for the controls advanced research turbine (CART). J Sol Energy Eng 2006;128(4):498–505.
[14] Laks J, Pao L, Wright A, Kelley N, Jonkman B. Blade pitch control with preview wind measurements. In: Proceedings of 48th AIAA Aerospace Sciences Meeting, Orlando, FL, AIAA-2010-251; Jan. 2010.
[15] Dunne F, Pao L, Wright A, Jonkman B, Kelley N. Combining standard feedback controllers with feedforward blade pitch control for load mitigation in wind turbines. In: Proceedings of 48th AIAA Aerospace Sciences Meeting, Orlando, FL, AIAA-2010-250; Jan. 2010.
[16] Schlipf D, Kuhn M. Prospects of a collective pitch control by means of predictive disturbance compensation assisted by wind speed measurements. In: Proc. German Wind Energy Conference (DEWEK), Bremen, Germany.
[17] Camblong Haritza, Nourdine Said, Vechiu Ionel, Tapia Gerardo. Comparison of an island wind turbine collective and individual pitch LQG controllers designed to alleviate fatigue loads. IET Renew Power Gener 2012;6(4):267–75.
[18] Medjber Ahmed, Guessoum Abderrezak, Belmili Hocine, Mellit Adel. New neural network and fuzzy logic controllers to monitor maximum power for wind energy conversion system. Energy 2016;106:137–46.
[19] Yin Xiu-xing, Lin Yong-gang, Li Wei, Ya-jing Gu, Liu Hong-wei, Lei Peng-fei. A novel fuzzy integral sliding mode current control strategy for maximizing wind power extraction and eliminating voltage harmonics. Energy 2015;85:677–86.
[20] Yang Bo, Jiang Lin, Wang Lei, Yao Wei, Wu QH. Nonlinear maximum power point tracking control and modal analysis of DFIG based wind turbine. Int J Electr Power Energy Syst 2016;74:429–36.
[21] Fantino Roberto, Solsona Jorge, Busada Claudio. Nonlinear observer-based control for PMSG wind turbine. Energy 2016;113:248–57.
[22] Behjat Vahid, Hamrahi Mehrdad. Dynamic modeling and performance evaluation of axial flux PMSG based wind turbine system with MPPT control. Ain Shams Eng J 2014;5(4):1157–66.
[23] Qais Mohammed H, Hasanien Hany M, Alghuwainem Saad. Enhanced salp swarm algorithm: Application to variable speed wind generators. Eng Appl Artif Intell 2019;80:82–96.
[24] Qais Mohammed, Hasanien Hany M, Alghuwainem Saad. Salp swarm algorithm-based TS-FLCs for MPPT and fault ride-through capability enhancement of wind generators. ISA Trans 2020;101:211–24.
[25] Soliman Mahmoud A, Hasanien Hany M, Azazi Haitham Z, El-kholy Elwy E, Mahmoud Sabry A. Hybrid ANFIS-GA-based control scheme for performance enhancement of a grid-connected wind generator. IET Renew Power Gener 2018;12(7):832–43.
[26] Soliman Mahmoud A, Hasanien Hany M, Al-Durra Ahmed, Alsaidan Ibrahim. A novel adaptive control method for performance enhancement of grid-connected variable-speed wind generators. IEEE Access 2020;8:82617–29.
[27] Mahmoud Hassan Y, Hasanien Hany M, Besheer Ahmed H, Abdelaziz Almoataz Y. Hybrid cuckoo search algorithm and grey wolf optimiser-based optimal control strategy for performance enhancement of HVDC-based offshore wind farms. IET Gener Transmiss Distrib 2020;14(10):1902–11.
[28] Jena Debashisha, Rajendran Saravanakumar. A review of estimation of effective wind speed based control of wind turbines. Renew Sustain Energy Rev 2015;43:1046–62.
[29] Moradi Hamed, Vossoughi Gholamreza. Robust control of the variable speed wind turbines in the presence of uncertainties: A comparison between and PID controllers. Energy 2015;90:1508–21.
[30] Gosk A. Model predictive control of a wind turbine [Master thesis]. Denmark, August: Technical University of Denmark; 2011.
[31] Henriksen LC. Model predictive control of wind turbines [PhD Thesis]. Technical University of Denmark; 2011.
[32] Korber A, King R. Model predictive control for wind turbines. In: Proceedings of European Wind Energy Conference.
[33] Korber A, King R. Nonlinear model predictive control for wind turbines. In: Proceedings of European Wind Energy Conference.
[34] Soliman Mostafa, Malik OP, Westwick David T. Multiple model predictive control for wind turbines with doubly fed induction generators. IEEE Trans Sustain Energy 2011;2(3):215–25.
[35] Schlipf David, Schlipf Dominik Johannes, Kuhn Martin. Nonlinear model predictive control of wind turbines using LIDAR. Wind Energy 2013;16 (7):1107–29.
[36] Spencer Martin D, Stol Karl A, Unsworth Charles P, Cater John E, Norris Stuart E. Model predictive control of a wind turbine using short-term wind field predictions. Wind Energy 2013;16:417–34.
[37] Koerber A, King R. Combined feedback feedforward control of wind turbines using state- constrained model predictive control. IEEE Trans Control Syst Technol 2013;21:1117–28.
[38] Jain Achin, Schildbach Georg, Fagiano Lorenzo, Morari Manfred. On the design and tuning of linear model predictive control for wind turbines. Renew Energy 2015;80:664–73.
[39] Lasheen Ahmed, Saad Mohamed S, Emara Hassan M, Elshafei Abdel Latif. Continuous-time tube-based explicit model predictive control for collective pitching of wind turbines. Energy 2017;118:1222–33.
[40] Mayne David Q. Constrained model predictive control: Stability and optimality. Automatica 2000;36(6):789–814.
[41] Jonkman, Jason, Butterfield Sandy, Musial Walter, Scott George. Definition of a 5-MW reference wind turbine for offshore system development. Golde, CO: National Renewable Energy Laboratory. Technical Report No. NREL/TP-500-38060; 2009.
[42] Mirzaei Mahmood, Hansen Morten H. A LIDAR-assisted model predictive controller added on a traditional wind turbine controller. In: Proceedings of American Control Conference (ACC). p. 1381–6.
[43] Schlipf D, Trabucchi D, Bischoff O, Hofsass M, Mann J, Mikkelsen T, et al. Testing of frozen turbulence hypothesis for wind turbine applications with a scanning LIDAR system. In: Proceedings of Int. Symp. Advancement of Boundary Layer Remote Sensing. p. 1–4.
[44] Simley Eric, Pao Lucy Y, Frehlich Rod, Jonkman Bonnie, Kelley Neil. Analysis of wind speed measurements using continuous wave LIDAR for wind turbine control. In: Proceedings of the 49th AIAA Aerospace Sciences Meeting.
[45] Newman JF, Clifton A. An error reduction algorithm to improve lidar turbulence estimates for wind energy. Wind Energy Sci 2017;2(1):77.
[46] Ghorbani MA, Khatibi R, FazeliFard MH, Naghipour L, Makarynskyy O. Short-term wind speed predictions with machine learning techniques. Meteorol Atmos Phys 2016;128(1):57.
[47] Liu Jinqiang, Wang Xiaoru, Yun Lu. A novel hybrid methodology for short-term wind power forecasting based on adaptive neuro-fuzzy inference system. Renew Energy 2017;103:620–9.
[48] Wang Jidong, Fang Kaijie, Pang Wenjie, Sun Jiawen. Wind Power Interval Prediction Based on Improved PSO and BP Neural Network. Network 2017;1:2.
[49] Madhiarasan M, Deepa SN. Performance Investigation of Six Artificial Neural Networks for Different Time Scale Wind Speed Forecasting in Three Wind Farms of Coimbatore Region. Int J Innov Sci Res 2016;23(2):380–411.
[50] Yin C, Rosendahl L, Luo Zh. Methods to improve prediction performance of ANN models. Simulate Model Pract Theory 2003;11(3):211–22.
[51] Sultana W Razia, Sahoo Sarat Kumar, Sesha Saikiran K, Rajasekhar Reddy GRT, Harshavard- han Reddy P. A computationally efficient finite state model predictive control for cascaded multilevel inverter. Ain Shams Eng J 2016;7 (2):567–78.
[52] Kumar Manjeet. Optimal design of fractional delay FIR filter using cuckoo search algorithm. Int J Circuit Theory Appl 2018;46(12):2364–79.
[53] Kumar Manjeet. Fractional order FIR differentiator design using particle swarm optimization algorithm. Int J Numer Model Electron Networks Devices Fields 2019;32(2):e2514.
[54] Singh Sandeep, Ashok Alaknanda, Kumar Manjeet, Rawat Tarun Kumar. Adaptive infinite impulse response system identification using teacher learner based optimization algorithm. Appl Intell 2019;49(5):1785–802.
[55] Yadav Suman, Yadav Richa, Kumar Ashwni, Kumar Manjeet. Design of Optimal two-Dimensional FIR filters with Quadrantally symmetric properties using vortex search algorithm. J Circ Syst Comput 2020;29(10):2050155.
[56] Aggarwal Apoorva, Kumar Manjeet, Rawat Tarun K, Upadhyay Dharmendra Kumar. Optimal design of 2-D FIR digital differentiator using L_1 L 1-norm based cuckoo-search algorithm. Multidimension Syst Signal Process 2017;28 (4):1569–87.
[57] Araghi A, Roghani GH, Riahy O Carlson, Gros S. Enhancing the net energy of wind turbine using wind prediction and economic NMPC with high-accuracy nonlinear WT models. Renew Energy 2020;151:750–63.
[58] Song Dongran, Yang Yinggang, Zheng Songyue, Deng Xiaofei, Yang Jian, Su Mei, et al. New perspectives on maximum wind energy extraction of variable-speed wind turbines using previewed wind speeds. Energy Convers Manage 2020;206:112496.
[59] Kimaev Grigoriy, Ricardez-Sandoval Luis A. Nonlinear model predictive control of a multiscale thin film deposition process using artificial neural networks. Chem Eng Sci 2019;207:1230–45.
[60] Lawrynczuk Maciej. Neural networks in model predictive control. In: Intelligent Systems for Knowledge Management. Berlin, Heidelberg: Springer; 2009. p. 31–63.
[61] Wu Zhe, Rincon David, Christofides Panagiotis D. Process structure-based recurrent neural network modeling for model predictive control of nonlinear processes. J Process Control 2020;89:74–84.

[62] Chen Yujiao, Tong Zheming, Zheng Yang, Samuelson Holly, Norford Leslie. Transfer learning with deep neural networks for model predictive control of HVAC and natural ventilation in smart buildings. J Cleaner Prod 2020;254.
[63] Kassem Ahmed M. Neural predictive controller of a two-area load frequency control for interconnected power system. Ain Shams Eng J 2010;1(1):49–58.
[64] Marzband Mousa, Azarinejadian Fatemeh, Savaghebi Mehdi, Guerrero Josep M. An optimal energy management system for islanded microgrids based on multiperiod artificial bee colony combined with Markov chain. IEEE Syst J 2015.
[65] Jonkman, Jason Mark, Buhl Jr Marshall L. FAST User's Guide. Nat. Renew. Energy Lab, Golden, CO, USA. Tech. Rep. NREL/EL-500-38230; 2005.
[66] Oye S. Flex 4–Simulation of wind turbine dynamics. In: Proceedings of 28th IEA Meeting Experts, State Art Aeroel. Codes Wind Turbine Calculat.; 1996. p. 71–6.
[67] Bossanyi E. GH Bladed User Manual. Bristol, U.K.: GH & Partners Ltd.; 2003.
[68] Aggarwal Apoorva, Rawat TK, Kumar Manjeet, Upadhyay DK. Design of optimal band-stop FIR filter using L1-norm based RCGA. Ain Shams Eng J 2018;9(2):277–89.
[69] Zolfaghari Mahdi, Taher Seyed Abbas, Munuz David Vindel. Neural network-based sensorless direct power control of permanent magnet synchronous motor. Ain Shams Eng J 2016;7(2):729–40.
[70] Hemeida, Ashraf Mohamed, Awad Hassan Somaia, Ali Mohamed Al-Attar, Alkhalaf Salem, Mahmoud Moun- tasser Mohamed, et al. Nature- inspired algorithms for feed-forward neural network classifiers: A survey of one decade of research. Ain Shams Eng J; 2020.
[71] Rezk Hegazy, Hasaneen El-Sayed. A new MATLAB/Simulink model of triple-junction solar cell and MPPT based on artificial neural networks for photovoltaic energy systems. Ain Shams Eng J 2015;6(3):873–81.
[72] Shamshad A, Bawadi MA, Wan Hussin WMA, Majid TA, Sanusi SAM. First and second order Markov chain models for synthetic generation of wind speed time series. Energy 2005;30(5):693–708.
[73] Carpinone A, Langella R, Testa A, Giorgio M. Very short-term probabilistic wind power forecasting based on Markov chain models. In: Probabilistic Methods Applied to Power Systems (PMAPS), 2010 IEEE 11th International Conference on. p. 107–12.
[74] Zaki John F, Ali-Eldin Amr, Hussein Sherif E, Saraya Sabry F, Areed Fayez F. Traffic congestion prediction based on Hidden Markov Models and contrast measure. Ain Shams Eng J 2019.
[75] Hocaoglu FO, Gerek ON, Kurban M. The effect of Markov chain state size for synthetic wind speed generation. In: Probabilistic Methods Applied to Power Systems, 2008. PMAPS'08. Proceedings of the 10th International Conference on; 2008. p. 1–4.
[76] Jonkman Bonnie J, Buhl Jr, ML. TurbSim User's Guide: Revised February 2007 for Version 1.21. No. NREL/TP-500-41136. Golden, CO (United States): National Renewable Energy Lab. (NREL); 2007.
[77] Siebert, Nils. Development of methods for regional wind power forecasting [PhD Thesis]. Ecole Na- tionale Superieure des Mines de Paris; 2008.
[78] Bemporad A, Morari M, Ricker NL. Model Predictive Control Toolbox 3 - User's Guide. The Mathworks Inc; 2008. http://www.mathworks.com/access/helpdesk/help/toolbox/mpc/.

Mahum Pervez was born in Pakistan on January 5, 1993. She received the Engineering degree in Electrical Engineering from the University of Engineering & Technology Peshawar, in 2015. She holds a Masters Degree in Electronic Engineering from Ghulam Ishaq Khan Institute of Engineering Sciences and Technology Topi, Pakistan in year 2017. She is currently a Lecturer in the Department of Electrical Engineering in University of Engineering & Technology Mardan since 2019. From 2017 to 2018, she worked as a Research Associate in Center of Intelligent Systems & Networks Research CISNR. Her research interests include renewable energy, advance control, embedded systems, power system control and artificial intelligence.

Tariq Kamal holds doctorates in energy and sustainability engineering from the University of Cadiz, Spain; and in electrical power and control engineering from the Sakarya University, Turkey. His research interests include advanced intelligent control techniques for power systems, hybrid renewable energy systems, plug-in hybrid electric vehicles, distributed generation and smart grid applications. Currently, he is working at the department of chair of renewable and sustainable energy systems, Technical University of Munich, Germany. He is the author/co-author of more than 70 papers published in various international scientific journals and conference proceedings. He has been involved in major joint projects around the globe.

Luis M. Fernández-Ramírez received Ph.D. degree in industrial engineering from the University of Cadiz, Cadiz, in 2004. From 1997 to 2000, he was with the Department of Development and Research, Desarrollos Eolicos S.A., Seville. In 2000, he joined the University of Cadiz, where he is currently an Associate Professor with the Department of Electrical Engineering and the Head of the Research Group in Electrical Technologies for Sustainable and Renewable Energy (PAIDI-TEP023). His current research interests include renewable energy sources, energy storage systems, hydrogen and fuel cell systems, electric vehicles, smart grids, power converters, and energy management/control systems.